UCRL-ID-119720

# Expedited Demonstration of Molten Salt Mixed Waste Treatment Technology

**Erica H. von Holtz**
**Robert W. Hopper**
**Martyn G. Adamson**

**February 2, 1995**

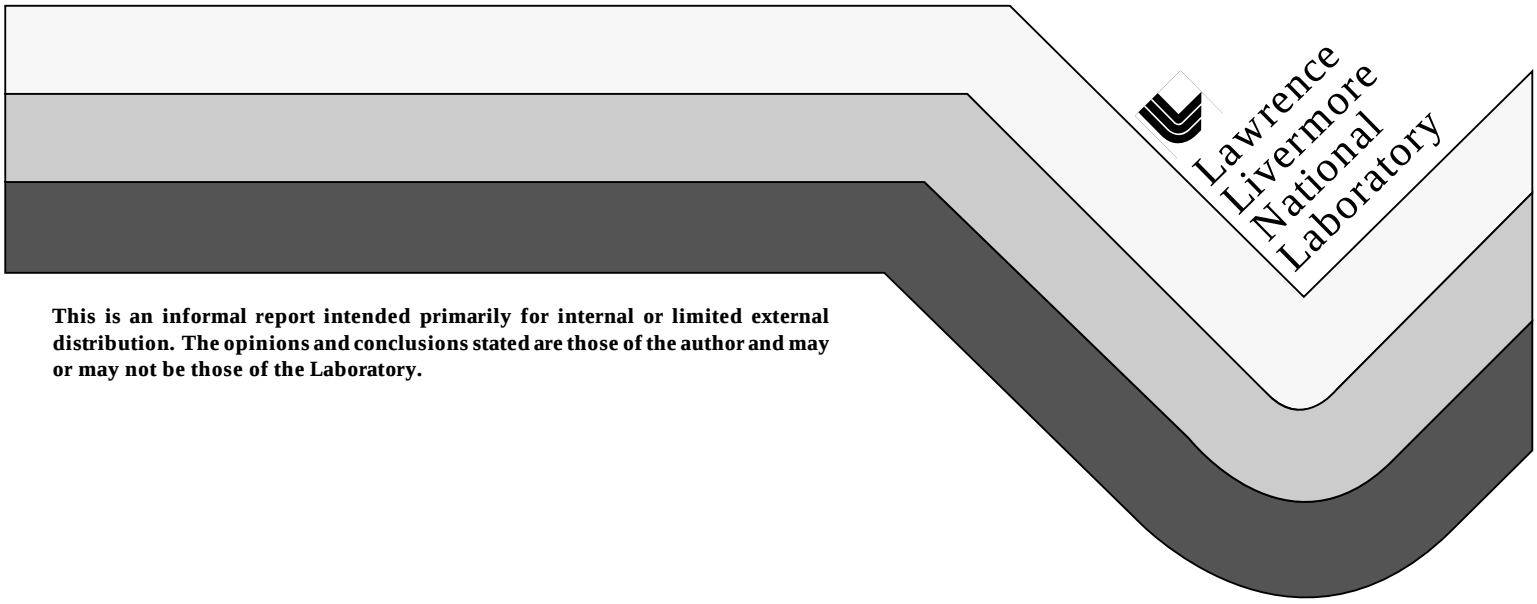

# Expedited Demonstration of Molten Salt Mixed Waste Treatment Technology
# LLNL TTP SF-2410-03 (Rev. 1)

## Final Report

### Executive Summary

### Subtask 1. Carbon Monoxide Emissions

Performance Metric

No current limitation exists for CO emissions for thermal treatment of hazardous waste, although EPA's proposed BIF standards of a limit of 100 ppm CO on a one-hour rolling average is a good basis upon which to compare MSO emissions. Success would be the establishment of a salt recycle schedule and/or a strategy for off-gas control for MWMF that keeps CO emissions below 100 ppm on an hourly averaged basis.

Results

Although CO emissions are dependent upon a number of factors – smooth versus pulsed delivery of the feed material, atomization of the fuel in the downcomer, mixing of fuel and oxidant air prior to salt entry, etc. – emissions will most likely meet this proposed standard when an excess of 20% air is used at chloride levels up to 20 mole percent. We have therefore selected 20 mol% as the baseline for the design of the MWMF salt recycle unit. Higher levels of NaCl build-up, up to 30 mol%, may be acceptable for some materials, such as methanol, methyl ethyl ketone, and ethylene glycol, and should be evaluated on a case-by-case basis.

### Subtask 2. Salt Melt Viscosity

Performance Metric

LLNL will perform experiments to determine salt viscosity as a function of ash composition, ash concentration, temperature, and time. These experiments will also discern whether or not there is a critical ash loading above which the salt will freeze in the vessel and not be readily removable by remelting. These experiments will enable us to establish a salt recycle schedule for MWMF based upon ash content, and provide information pertinent to heater design, in the event of emergency shut-down, to remelt ash-bearing salt. Attainment of this goal will constitute success for this technical issue.

Results

The dip cup viscosity technique chosen for this work is simple and inexpensive, and yielded good results with salts of low viscosity. Because of the unexpectedly viscous nature of many of the salt compositions specified for this subtask, the test method did not perform to our satisfaction. Further work is suggested, in which the experimental procedure would be modified as follows. First, detailed analysis of real ash should be done to fully characterize the particle size distribution and surface area to enable better surrogates to be chosen. A viscometer of the rotating spindle type should be used, requiring the fabrication of platinum spindles, since the standard Brookfield set-up cannot be used at the temperatures specified herein. Lastly, the apparatus should have the capability to provide a partial $CO_2$ atmosphere, with the salt composition monitored via DTA-TGA, to eliminate $CO_2$ loss from decomposition.

**Subtask 3. Sodium Carbonate Volatility**

Performance Metric

Success for this task would be the determination that the amount of sodium carbonate entrained in the off-gas is minimal, and that any deposited salt can easily be removed from the piping using a soot blower or other means. A minimum result is assurance that MSO pilot plant operation is practical ($10^2$ to $10^3$ hours). A preferred result is that an MSO pilot plant can operate for practical periods ($10^3$ to $10^4$ hours) without shutdowns for cleanout.

Results

The amount of carryover has been measured, and has been found to increase with the amount of sodium chloride present and the superficial velocity. The amount of carryover can be mitigated via the use of baffles. First, the baffles will form a tortuous path for the exhaust gas to follow, which will deter particles from following a simple line-of-sight to the exhaust exit. Second, baffles located in the upper portion of the reactor can be designed as a heat sink, minimizing the vapor carryover as well. ETEC has successfully demonstrated the effectiveness of baffles; work will soon be underway to design and demonstrate baffles for the MWMF MSO system. The salt which was entrained in the off-gas and deposited in pipe sections with steel wool filters was easily removed, indicating that the use of a soot blower will easily remove any carryover from the exhaust pipes. By utilizing baffles and periodically operating a soot blower, MSO pilot plant operation for periods on the order of $10^3$ hours without shutdowns for cleanout of off-gas pipes should be practical.

**Subtask 4. Final Forms**

Performance Metric

Success for this task would be the provision of at least one final waste form that meets the waste acceptance criteria (WAC) of a landfill that will take the waste. If several forms meet this condition, then data useful for choosing between them for a given treatment environment should have been obtained or at least identified.

Results

TCLP leach results available at this time did not meet the necessary criteria for land disposal. However, our views on the advantages of this waste form for MSO salt remain unchanged: it provides a high-quality waste form with good salt loadings at reasonable costs. Twin-screw extrusion is technically preferable to single-screw, though more expensive. Good dispersion of the salt in the LDPE was achieved in this study. The inherent immobilization achievable by microencapsulation (i.e., ignoring any chemical pre-conditioning of the waste) requires further investigation. The effect of particle size will be evaluated when the remaining data of this project are in hand. The volumetric loading levels at which leach resistance began to deteriorate were disappointingly low. It is believed, however, that continued process innovation and optimization will lead to significantly better combinations of loading and immobilization.

## 1. Carbon Monoxide Emissions

Task Objective

A variety of PICs (Products of Incomplete Combustion) may be found in off-gas streams from all thermal processes (e.g., incineration, MSO, etc.). Air quality regulations for incinerators infer that the amount of carbon monoxide (CO) evolved is a direct indication of the level of other PICs present in the off-gas as well. While it is not clear that this same inference is valid for MSO, the minimization of CO is certainly desirable for any process. For MSO, CO may be present in the off-gas above the acceptable limits (as proposed for incineration) when chlorine is in the waste. Available evidence indicates that the formation of CO may be affected by a number of factors, including the composition of the melt (in particular chloride content), the process stoichiometry, temperature and throughputs, and the hydrodynamics of the MSO vessel. The effect of chloride content on CO production needs to be evaluated jointly with the formation of PICs in the off-gas.

Experimental Methodology and Results

The specific feed materials used encompassed a wide variety of organics. We selected an alcohol and a ketone commonly used as cleaning agents, methanol and methyl ethyl ketone. We also chose an aromatic compound, toluene, which is a commonly used solvent in scintillation cocktails. Lastly, we chose mineral oil as representative of the inventory of waste oils. We were unable to run pure mineral oil because it was too viscous for our pump; a 50/50 solution (by weight) of mineral oil and toluene has been run for all tests. Non-halogenated materials were selected to maintain a constant chloride content in the melt during each series of tests. Target flow rates for the feed materials and oxidant air were calculated based on achieving an apparent velocity of 1 ft./s through the reactor, using 120% stoichiometric air. Sodium carbonate was the baseline salt used, and was doped with 10, 20, and 30 mole percent sodium chloride to study the effect of chloride content in the melt.

Initial results reported in our 12/1/94 Interim Summary Memorandum of Findings used an injector which featured active and passive cooling of the feed material, which was done because of the low flash points of several of the test materials. Oxidant air was injected through a separate tube in the salt bed. As evidenced by the CO emissions seen, good mixing was not occurring with this method. After consultation with Energy Technology Engineering Center (ETEC) and Oak Ridge National Laboratory (ORNL), we fabricated an injector of their design. With this type of injector, the feed material is pumped down the inner of two concentric tubes (0.64 and 1.27 cm in diameter, respectively) along with 5.7 SLPM of air (approximately 10% of the total input oxidant air). The balance of the oxidant air is fed through the outer tube. Both of those tubes are encased by a 3.8-cm-diameter pipe, which extends approximately 25 cm further than the inner tubes. Upon exit of the inner tubes, all air mixes intimately with the feed material in that 25 cm zone prior to entrance into the molten salt. After a brief study of the effect of injector depth, the bottom of the 3.8-cm-diameter tube was positioned approximately 2.5 cm from the bottom of the vessel for all tests reported herein. (Different materials of construction than those used by ETEC and ORNL were used based on stock

availability at LLNL.) To evaluate the effectiveness of this injector design, compared to the injector initially used, ethylene glycol was run through the reactor. (Ethylene glycol was chosen because it was used by ORNL as a diluent for their feed materials, and comparative data exists.) Our first tests compared favorably with results seen at ORNL, and we then ran our target rates for the three materials reported on in the interim summary. The data for the two types of injectors is shown in Table 1.1. It is clear from this data that the injector configuration is a critical parameter in the design of an efficient MSO unit; good mixing of the feed material and oxidant air must occur before entrance into the molten salt.

**Table 1.1: Comparison of CO Evolutions for Different Injectors**

| | Cooling Injector | | | Coaxial Injector | | |
|---|---|---|---|---|---|---|
| **Feed Material** | **Feed Rate (g/min.)** | **Air Flow (SLPM)** | **Avg. CO (ppm)** | **Feed Rate (g/min.)** | **Air Flow (SLPM)** | **Avg. CO (ppm)** |
| MEK | 5.9 | 61.7 | 73 ± 14 | 6.3 | 57.6 | 1 ± 7 |
| Toluene | 4.9 | 63.9 | 166 ± 21 | 5.9 | 63.7 | 0 ± 3 |
| Mineral Oil/Toluene | 3.5 | 62.9 | 238 ± 33 | 5.5 | 62.9 | 2 ± 3 |

A slipstream of the off-gas was diverted past a cold trap, silica wool filter, and was then split into two streams. The first stream was analyzed for CO concentration by passing it through both a Horiba VIA-510 and a Horiba PIR-2000 infrared gas analyzers. These two units were set to ranges of 0 – 1000 ppm and 0 – 5%, respectively. All steady state results reported were obtained using the VIA-510, which has an accuracy of ± 1%. The latter analyzer was only used to measure start-up emissions, which at times exceeded 1000 ppm, and during optimization studies. The second stream was sent through a mass spectrometer (MS). The MS was used solely to determine the $CO_2$ and $O_2$ concentrations in the outlet gas since masking of many other peaks of interest occurred with the high levels of nitrogen present in air. However, the real-time data observed for $CO_2$ and $O_2$ was invaluable for monitoring the progress of the run and determining when steady-state had been reached.

We deviated from the original test plan in three ways. First, since data was obtained for ethylene glycol during the initial evaluation of the coaxial injector, this material was added to the matrix of materials tested at all levels of chloride content. Second, we did not run each steady state test for 2 hours. We found that steady state was achieved within 10 – 15 minutes of the start of the run, and was extremely stable as evidenced by the small standard deviations seen with the MS. Because of this stability, and because of the time frame involved for the completion of the tests, the duration of each experiment was cut to an average of 52 minutes. Lastly, we did not run individual tests for 880 and 950°C, but collected data over the temperature range from between 860–880°C and 950–960°C. We found, contrary to expectations, that CO emissions were essentially independent of temperature for the materials tested. This is plotted for four representative tests in Figure 1.1. (The high CO data point shown for the ethylene glycol run is believed to be an artifact of start-up.) Results

reported herein are therefore reported as valid for the temperature range of 880–950°C, rather than for a discrete temperature.

**Figure 1.1: CO Evolution as a Function of Temperature**

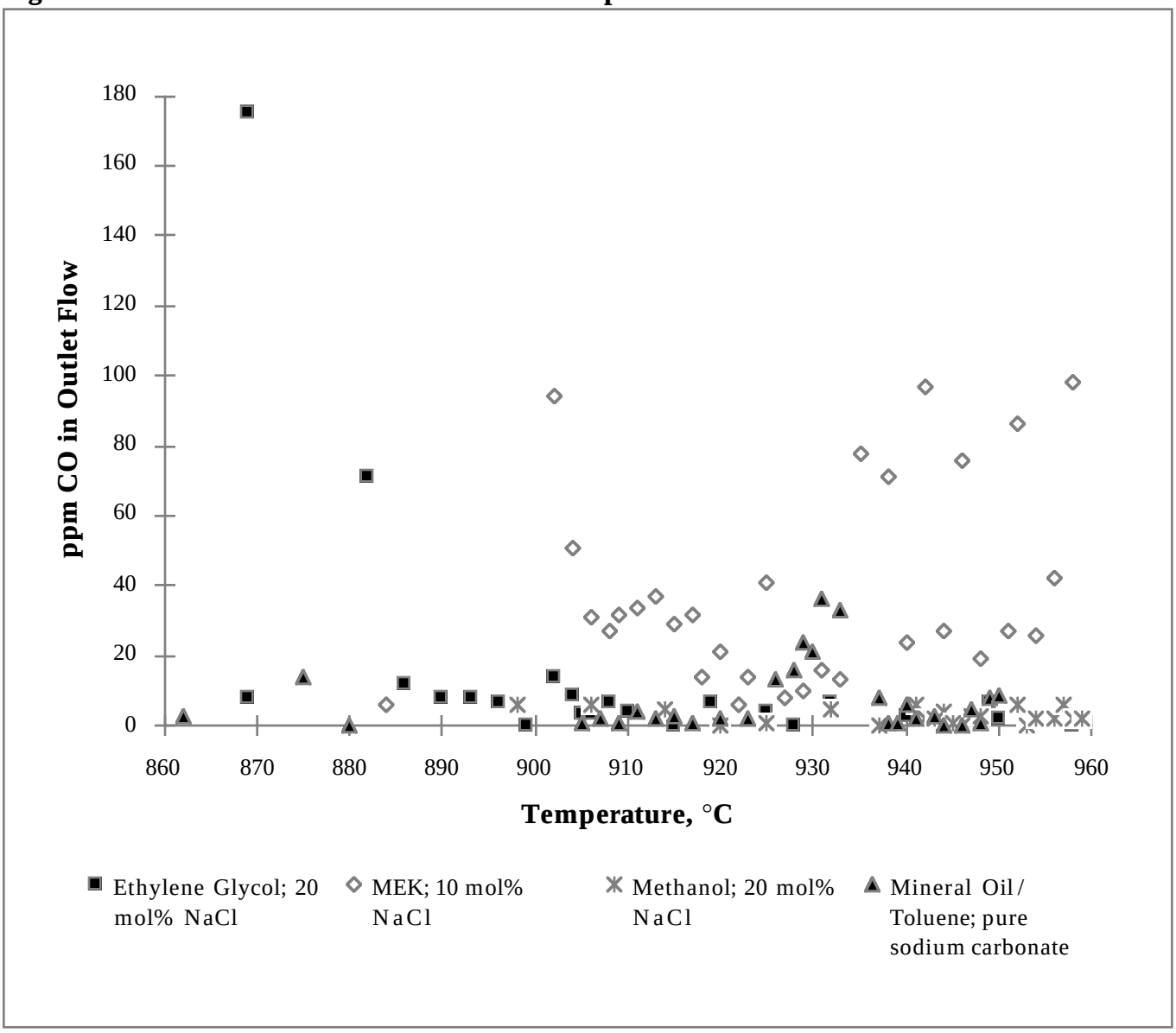


Steady state results are reported in Tables 1.2 – 1.6 for ethylene glycol, methanol, methyl ethyl ketone, toluene, and a mixture of 50 wt% mineral oil and 50 wt% toluene, respectively. Again, target flow rates for the feed materials and oxidant air were based on achieving a superficial velocity ($V_S$) of 1 ft./s through the reactor, using 120% stoichiometric air, with the exception of ethylene glycol. The target for ethylene glycol was 0.8 ft./s and 180% stoichiometric air, which approximates the conditions used at ORNL. In fact, less than 160% of the stoichiometrically required air was used for the ethylene glycol runs. Based on the actual flow rates of feed

materials obtained, experiments using methyl ethyl ketone, toluene, and the mineral oil/toluene mixture were all conducted with less than 120% excess air, with superficial velocities ranging between 1.00–1.08 feet per second. The supplying of less than 20% excess air was caused by an error in an Excel spreadsheet, which was discovered after the initiation of the test plan. Rather than change the experiments in the middle of the test matrix, material and air feed rates were maintained to enable evaluation of CO results for comparable test conditions.

**Table 1.2: Summary for Ethylene Glycol Runs**

| mol% NaCl | Feed Rate (g/min.) | Avg. CO (ppm) | Avg. $CO_2$ (Dry Basis) (%) | Avg. $O_2$ (Dry Basis) (%) | $V_s$ (ft./s) | % Stoich. air used | % C converted to CO |
|---|---|---|---|---|---|---|---|
| 0 | 7.00 | 0 ± 3 | 7.41 ± 0.04 | 11.44± 0.10 | 0.87 | 159.7 | <0.01 |
| 10 | 7.10 | 5 ± 3 | 8.08 ± 0.13 | 11.97 ± 0.08 | 0.87 | 157.5 | <0.01 |
| 20 | 7.48 | 4 ± 4 | 7.33 ± 0.04 | 11.82 ± 0.04 | 0.88 | 149.5 | <0.01 |
| 30 | 7.00 | 73 ± 29 | 9.15 ± 0.01 | 9.94 ± 0.01 | 0.87 | 159.7 | 0.07 |

All ethylene glycol experiments 48.1 SLPM oxidant air.

**Table 1.3: Summary for Methanol Runs**

| mol% NaCl | Feed Rate (g/min.) | Avg. CO (ppm) | Avg. $CO_2$ (Dry Basis) (%) | Avg. $O_2$ (Dry Basis) (%) | $V_s$ (ft./s) | % Stoich. air used | % C converted to CO |
|---|---|---|---|---|---|---|---|
| 0 | 7.42 | 1 ± 4 | 7.14 ± 0.05 | 11.00 ± 0.09 | 1.07 | 152.7 | <0.01 |
| 10 | 7.66 | 3 ± 3 | 10.02 ± 0.03 | 7.01 ± 0.03 | 1.08 | 147.8 | <0.01 |
| 20 | 7.63 | 2 ± 3 | 7.42 ± 0.05 | 9.60 ± 0.04 | 1.08 | 148.3 | <0.01 |
| 30 | 7.84 | 4 ± 3 | 10.08 ± 0.27 | 8.00 ± 0.03 | 1.08 | 144.4 | <0.01 |

All methanol experiments 56.6 SLPM oxidant air.

**Table 1.4: Summary for Methyl Ethyl Ketone Runs**

| mol% NaCl | Feed Rate (g/min.) | Avg. CO (ppm) | Avg. $CO_2$ (Dry Basis) (%) | Avg. $O_2$ (Dry Basis) (%) | $V_s$ (ft./s) | % Stoich. air used | % C converted to CO |
|---|---|---|---|---|---|---|---|
| 0 | 6.30 | 1 ± 7 | 10.61 ± 0.45 | 6.34 ± 0.05 | 1.00 | 112.3 | <0.01 |
| 10 | 6.31 | 19 ± 11 | 10.40 ± 0.09 | 7.25 ± 0.04 | 1.00 | 112.1 | 0.01 |
| 20 | 6.34 | 63 ± 8 | 10.90 ± 0.11 | 6.16 ± 0.13 | 1.00 | 111.5 | 0.04 |
| 30 | 6.20 | 86 ± 26 | 13.59 ± 0.10 | 3.90 ± 0.05 | 1.00 | 114.1 | 0.06 |

All MEK experiments 57.6 SLPM oxidant air.

**Table 1.5: Summary for Mineral Oil/Toluene Runs**

| mol% NaCl | Feed Rate (g/min.) | Avg. CO (ppm) | Avg. $CO_2$ (Dry Basis) (%) | Avg. $O_2$ (Dry Basis) (%) | $V_s$ (ft./s) | % Stoich. air used | % C converted to CO |
|---|---|---|---|---|---|---|---|
| 0 | 5.49 | 2 ± 3 | 8.58 ± 0.04 | 9.39 ± 0.06 | 1.06 | 103.9 | <0.01 |
| 10 | 5.32 | 210 ± 19 | 13.43 ± 0.03 | 3.32 ± 0.06 | 1.06 | 107.3 | 0.14 |
| 20† | 5.35 | 134 ± 38 | 13.37 ± 0.07 | 2.76 ± 0.01 | 1.06 | 106.7 | 0.09 |
| 30 | 5.45 | 532 ± 93 | 14.17 ± 0.06 | 2.34 ± 0.16 | 1.06 | 104.7 | 0.35 |

All mineral oil/toluene experiments used 62.9 SLPM oxidant air.

†The Mass Spectrometer data collection terminated mid-run; $CO_2$ and $O_2$ percentages were taken manually and are on a wet basis for this run only.

**Table 1.6: Summary for Toluene Runs**

| mol% NaCl | Feed Rate (g/min.) | Avg. CO (ppm) | Avg. $CO_2$ (Dry Basis) (%) | Avg. $O_2$ (Dry Basis) (%) | $V_s$ (ft./s) | % Stoich. air used | % C converted to CO |
|---|---|---|---|---|---|---|---|
| 0 | 5.48 | 0 ± 3 | 11.43 ± 0.03 | 6.10 ± 0.04 | 1.06 | 111.4 | <0.01 |
| 10 | 5.34 | 51 ± 21 | 13.03 ± 0.09 | 4.77 ± 0.03 | 1.06 | 114.3 | 0.03 |
| 20 | 5.38 | 66 ± 24 | 13.29 ± 0.03 | 3.77 ± 0.02 | 1.06 | 113.5 | 0.04 |
| 30 | 5.38 | 276 ± 79 | 13.25 ± 0.04 | 3.82 ± 0.03 | 1.06 | 113.5 | 0.18 |

All toluene experiments used 63.7 SLPM oxidant air.

The CO emissions for each feed material are plotted as a function of the mole percent of NaCl in Figure 1.2. The following conclusions can be drawn from this graph. First, CO emissions do increase as the concentration of sodium chloride in the melt increases, with an anomaly noted for the mineral oil/toluene mixture at 10 mol% NaCl. (Other differences seen in the progression from 10 to 20 mole percent are within the standard deviations of the CO measurements and are not significant.) Second, small oxygenated molecules are less affected by increases in chloride content than are ring compounds and long-chain molecules. Methanol, for example, showed no effect as the chloride content was increased; in fact, higher feed rates were put through the reactor as the NaCl content was increased with no effect on CO evolutions. Ethylene glycol, methanol, and methyl ethyl ketone at the conditions tested all produced less than 100 ppm of CO on a rolling average. Toluene experiments produced less than 100 ppm CO when 20 mol% sodium chloride and less is present in the melt; mineral oil/toluene experiments produced less than 100 ppm CO only for the pure sodium carbonate experiments.

It should again be noted that all experiments with methyl ethyl ketone, mineral oil/toluene, and toluene were all run under less than ideal conditions, using less than 20% excess air because of the calculation error. The effect of this error is shown graphically in Figure 1.3, in which CO emissions are plotted as a function of percent stoichiometric air used for each feed material. Less than 8% excess air was used in the mineral oil/toluene experiments; a significant reduction of CO generation is

**Figure 1.2: Evolution of CO as a Function of NaCl Content**

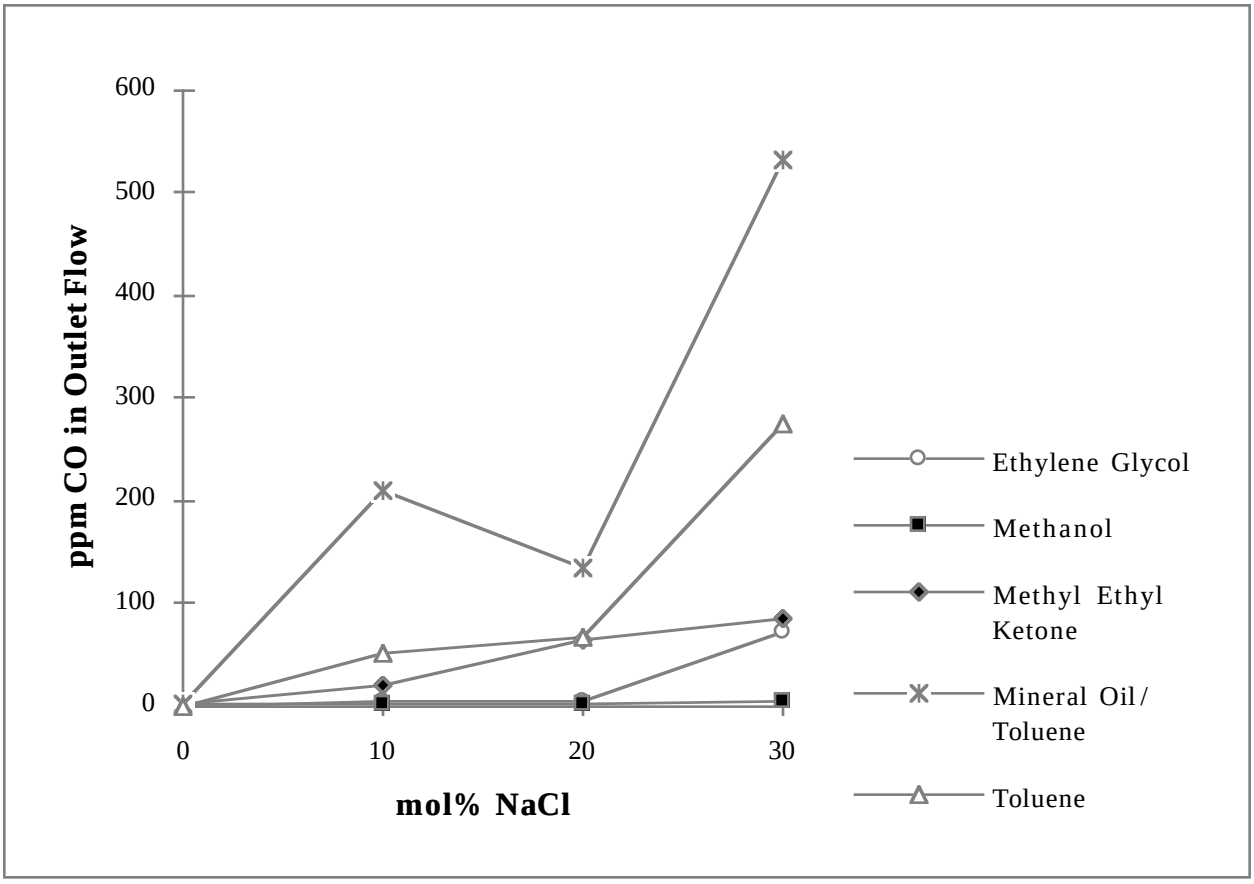


expected as the excess air is increased to 20%. Only 11 – 14% excess air was used in the methyl ethyl ketone and toluene experiments. Again, increasing the air/fuel ratio to 120% would reduce the CO emissions seen for these two materials. The ethylene glycol runs were purposely made using between 50 – 60% excess air, to match ORNL run conditions. Methanol experiments, on the other hand, used between 144 – 153% stoichiometric air because of the error in the pre-experiment calculations. It is expected that a reduction in the amount of air, to 20% excess, would not impact CO emissions significantly.

Figure 1.4 shows the percentage of carbon in the feed material that was converted to CO, as a function of chloride content in the melt. All methanol experiments, with the high amount of excess air used, resulted in less than 0.01% conversion. (That level of conversion, which results in less than 10 ppm CO, is the limit of accuracy of the calculations.) The percentage of carbon converted to CO does not exceed 0.10% until the chloride content exceeds 20 mol% NaCl, with the exception of the anomaly noted early for mineral oil/toluene at 10 mol% NaCl. Ethylene glycol and methyl ethyl ketone experiments never exceeded 0.10% conversion, even at the upper chloride contents. The difficulty in oxidizing the ring and long-chain compounds is again evidenced in Figure 1.4 with the higher conversion of carbon in toluene and

**Figure 1.3: CO Emissions as a Function of Stoichiometric Air**

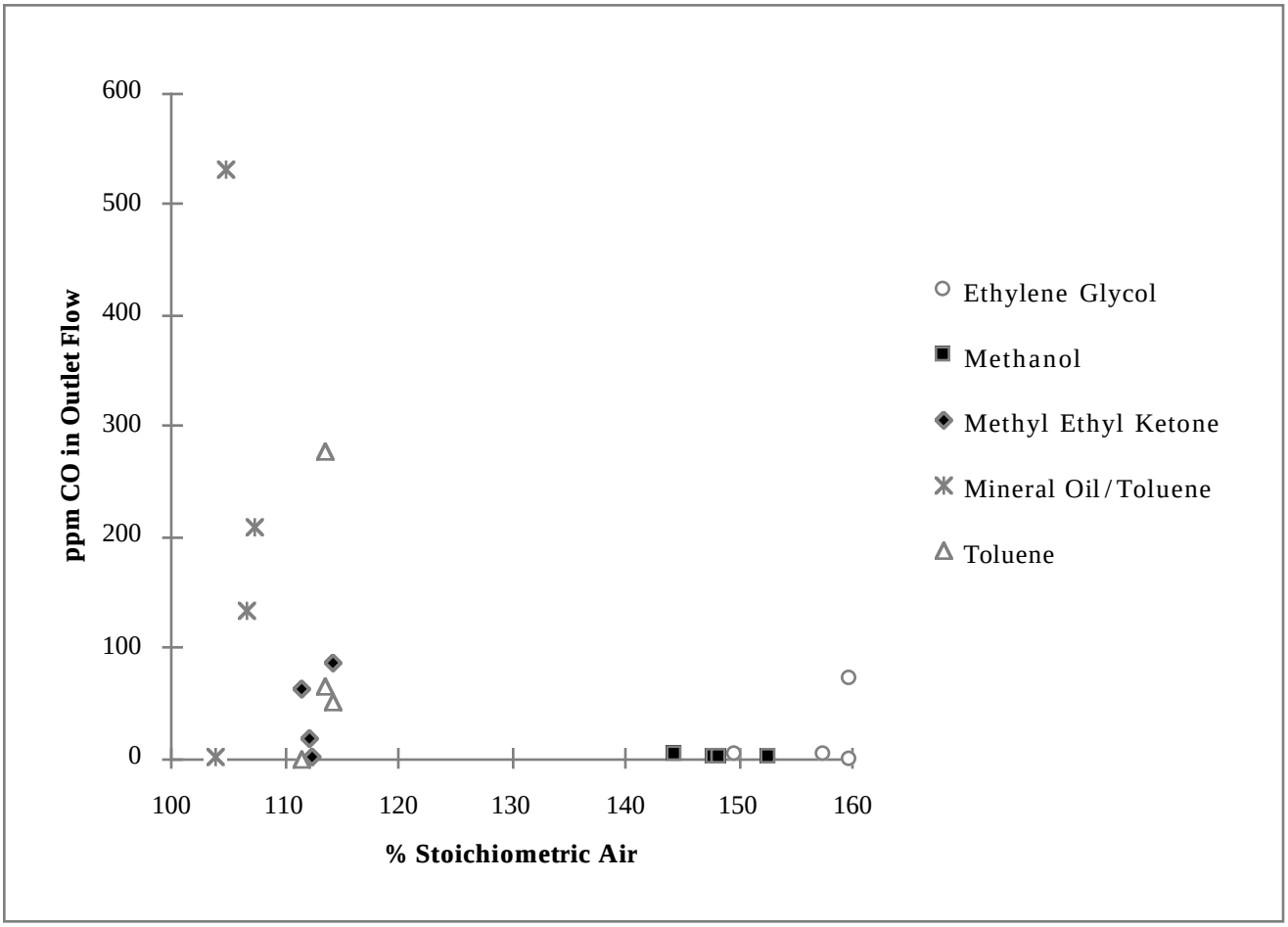


mineral oil to CO at the 30 mol% NaCl levels. However, the level of conversion is expected to decrease for both mineral oil and toluene when the amount of excess air is increased to the desired level of 20%.

If CO is formed during the oxidation process, either in the downcomer or in the salt bed, it is extremely difficult to convert this CO to $CO_2$ because this reaction is very slow, even at high temperatures. To examine the conversion of CO to $CO_2$ in the MSO reactor, we used a gas standard that contained 2% CO, 10% $CO_2$, and 5% $O_2$, with the balance nitrogen. This standard was sent through the MSO unit at 880 and 950°C, varying the approximate residence time of the gas through the melt/froth region from 13 to 6.5 seconds ($V_s$ varied from 0.1 – 0.2 ft./s). The conversion of CO to $CO_2$ is tabulated in Table 1.7. As the residence time is reduced, the conversion of CO drops off quickly. However, this reaction is highly dependent upon temperature, with higher conversion seen as the temperature was increased from 880 to 950°C. Since current MSO units are designed to operate with throughputs of 1 – 2 ft./s, injector design will be critical to ensuring intimate mixing and avoidance of initial CO formation.

**Figure 1.4: % C Converted to CO as a Function of NaCl Content**

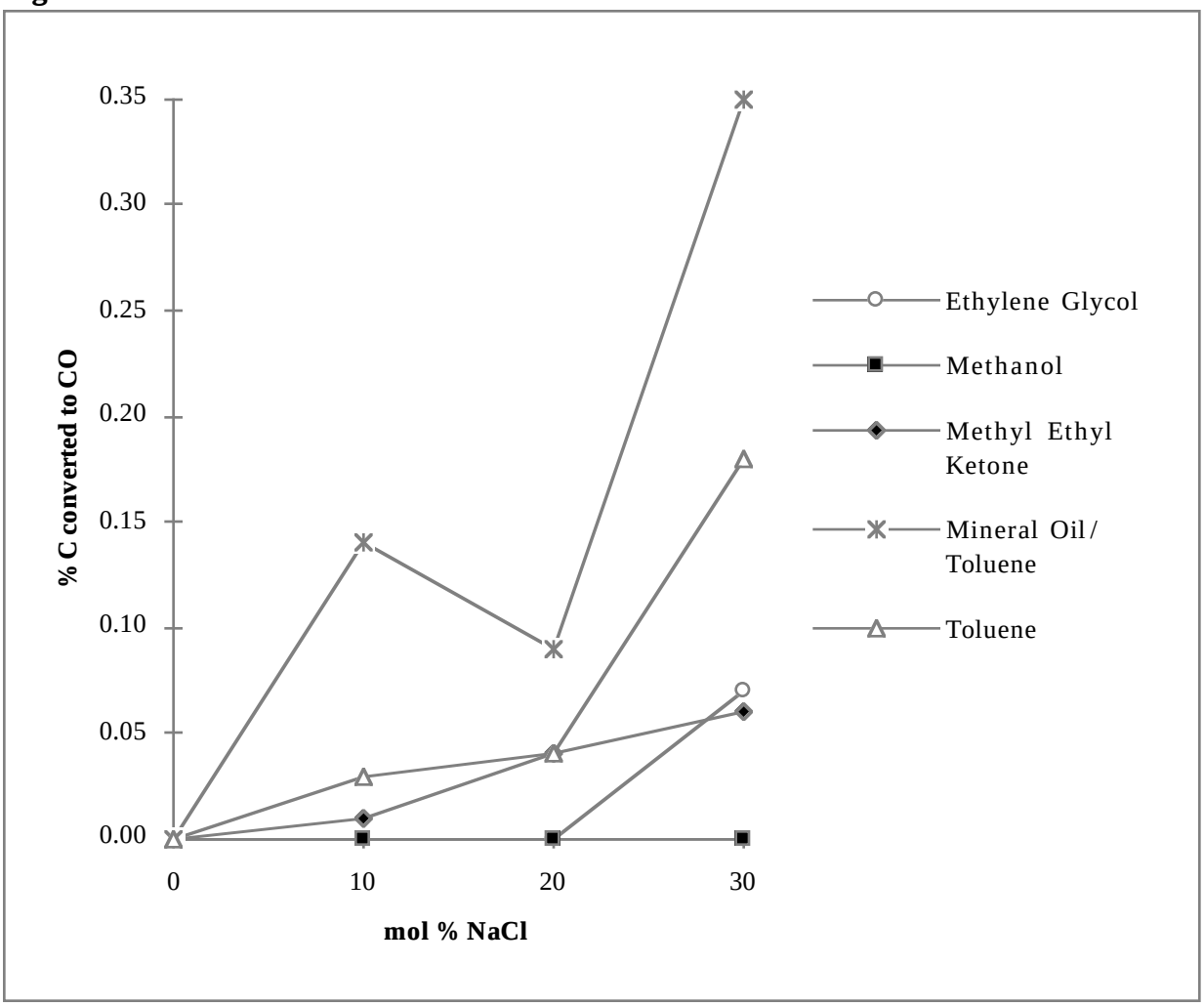


**Table 1.7: Conversion of CO to $CO_2$ as a Function of Residence Time**

| $V_s$ of Standard (ft./s) | Gas Flow (SLPM) | Temperature (°C) | % CO → $CO_2$ |
|---|---|---|---|
| 0.10 | 5.7 | 880 | 98.5 |
| 0.15 | 8.6 | 880 | 96.0 |
| 0.20 | 11.4 | 880 | 82.4 |
| 0.20 | 11.4 | 950 | 97.1 |

Performance Metric

No current limitation exists for CO emissions for thermal treatment of hazardous waste, although EPA's proposed BIF standards of a limit of 100 ppm CO on a one-hour rolling average is a good basis upon which to compare MSO emissions. Success would be the establishment of a salt recycle schedule and/or a strategy for off-gas control for MWMF that keeps CO emissions below 100 ppm on an hourly averaged basis.

Results

Although CO emissions are dependent upon a number of factors – smooth versus pulsed delivery of the feed material, atomization of the fuel in the downcomer, mixing of fuel and oxidant air prior to salt entry, etc. – emissions will most likely meet this proposed standard when an excess of 20% air is used at chloride levels up to 20 mole percent. We have therefore selected 20 mol% as the baseline for the design of the MWMF salt recycle unit. Higher levels of NaCl build-up, up to 30 mol%, may be acceptable for some materials, such as methanol, methyl ethyl ketone, and ethylene glycol, and should be evaluated on a case-by-case basis.

## 2. Salt Melt Viscosity

Task Objective

Salt melt and equilibrium issues have been identified with respect to the effect of ash content. The ash content will impact the melt viscosity and hydrodynamics, and may have an indirect impact on the destruction efficiency. A number of tests were conducted outside of the bench-scale MSO unit to evaluate the viscosity issue relative to concentration of ash, temperature of the melt, and time in solution.

Experimental Methodology and Results

Most paper-based waste streams contain kaolin, which is a hydrous aluminum silicate. A finding from an earlier LLNL study was that alumina or silica individually do not affect the viscosity to any large extent. It is only when these materials are present in a 1 to 1 proportion that the viscosity shows any appreciable rise, most likely resulting from the polymerization of the alumina and silica. Earlier LLNL and Rockwell experiments show that the viscosity of salt melts with 20 – 30% kaolinite at 800°C to 900°C was on the order of 10–40 centipoise, and increased steadily with time[1]. For this TTP, we investigated the viscous behavior of molten sodium carbonate at 880°C and 950°C containing a variety of ash surrogates. The test matrix called for using 100% alumina ($Al_2O_3$), 100% silica ($SiO_2$), and a 50-50 (molar) mixture of $Al_2O_3$ and $SiO_2$ as ash surrogates, in concentrations of 10, 20, 30 and 40% by weight.

Details of the previous LLNL experiments were not available; most of the staff involved have subsequently left the Laboratory. After considering a number of viscosity measurement techniques, it was determined that a modification of ASTM D 4212[2] would be best suited to the sodium carbonate measurements at 880° and 950°C since low viscosities were expected. In this procedure, a measurement is made of the time required to drain the test fluid through an orifice in a standard cup. Zahn cups are among the most commonly used devices of this type; for our tests several similar cups have been made from Inconel® 601 crucibles. The viscosity cups fabricated had orifices corresponding to Zahn cups No. 1 (0.1994 cm diameter), No. 3 (0.3797 cm diameter) and No. 5 (0.5309 cm diameter). Even though resulting data are expressed in units of time rather than conventional viscosity units, results would be comparable over the range of salt compositions tested. Any increase in viscosity is readily apparent using this method.

The test apparatus included an electric resistance-heated furnace, 20 cm ID by 30.5 cm high. Salt melts were prepared by blending the powders to insure homogeneity, and then melting them in a 750 mL alumina crucible located in the furnace. Secondary containment was provided by a 500 mL Inconel® 601 crucible. The viscosity cup was suspended just above the melt surface prior to the test so that it would reach equilibrium temperature, and remained in the furnace hot zone throughout the procedure. A hole cut through the side of the furnace permitted direct observation of the melt as it drained from the cup. A diagram of this set-up is shown in Figure 2.1.

The sodium carbonate used was from the same reagent grade lot used for the carbon monoxide emissions tests. Real ash is believed to have a particle size on the order of 0.1 μm, although the exact surface area (particle morphology) has not been measured by LLNL. The ash surrogates used were 45 μm (–325 mesh) silica, 0.7 μm alumina, and 45 μm (–325 mesh) kyanite (a 50-50 molar mixture of $Al_2O_3$ and $SiO_2$).

To calibrate the test assembly, initial tests were made at 20–21°C with deionized water, mineral oil, and Karo® light corn syrup. Karo® was chosen because a salt of that viscosity would clearly be unacceptable since small bubble formation is not attainable in a liquid with this high a viscosity. Results from the dip cups were compared with measurements using a Brookfield Model RVT-DV-1 viscometer with either spindle size 1 or 5. Calibration test results are summarized in Table 2.1, with median cup drain times in seconds and Brookfield measurements in centipoise. It should be noted that cup drain times are considered acceptable only if they are between 20 and 100 seconds; times shown for water through orifice number three and for Karo® syrup are outside this range.

**Table 2.1: Calibration Test Results**

| | Orifice Size | | | Brookfield |
|---|---|---|---|---|
| **Material** | **No. 1** | **No. 3** | **No. 5** | **Viscometer** |
| Deionized $H_2O$ | 34.3 s | 13.3 s | | -- |
| Mineral Oil | -- | 36.6 s | | 167 cp |
| Karo® Syrup | | | 223.2 s | 5840 cp |

Data subsequently taken for molten salt melts are listed in Table 2.2. Results within the acceptable range of time were only obtained using the smallest diameter orifice. It is observed that drain times for pure molten sodium carbonate are comparable to room temperature water, although slightly lower. Published data[3] gives the viscosity / temperature relationship for sodium carbonate as

$$\eta = 0.18937 \exp(\frac{28834.1}{RT}).$$

**Figure 2.1: Viscosity Test Apparatus**

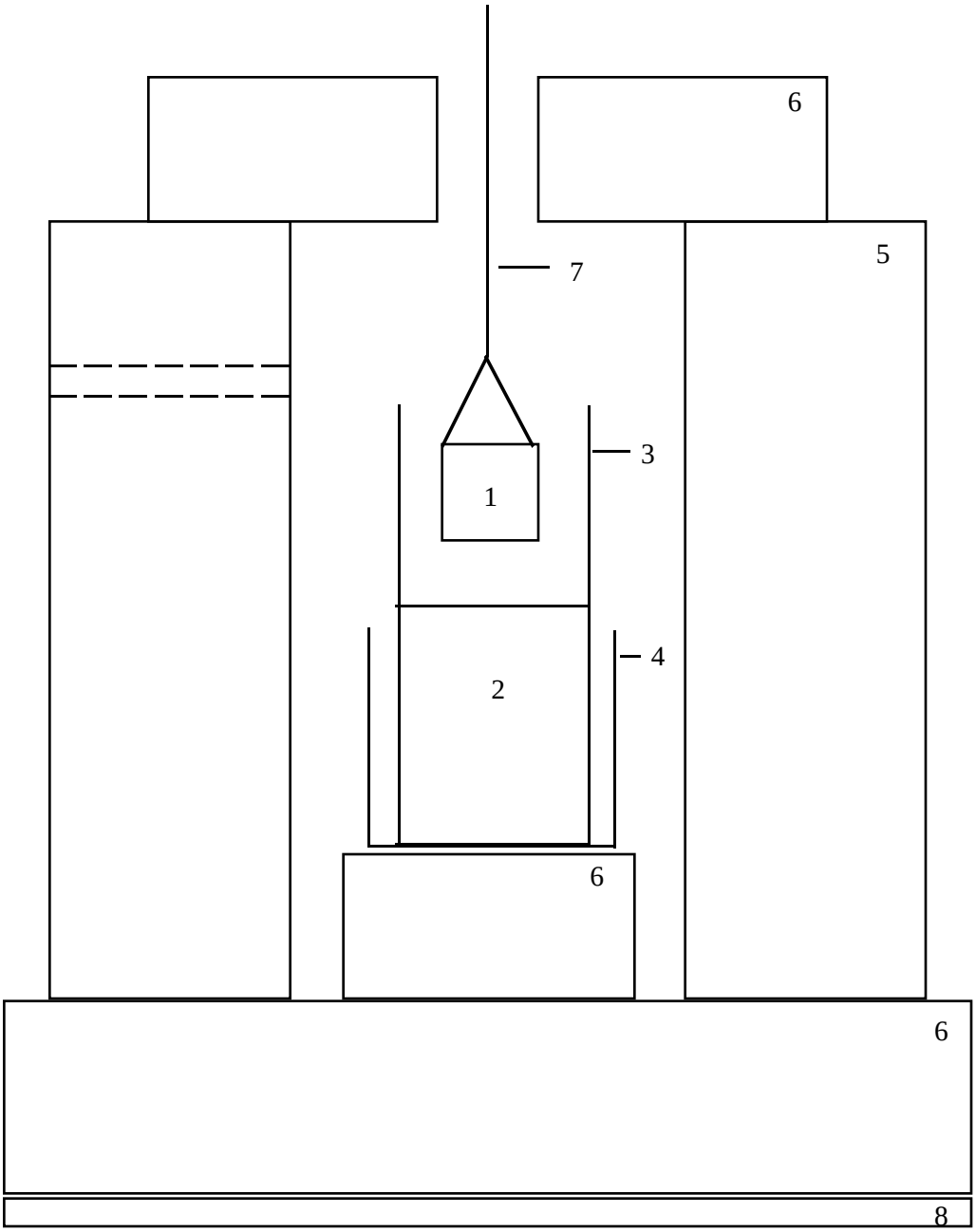


1. Dip Cup
2. Salt
3. Alumina Crucible
4. Inconel Secondary Containment Crucible
5. Fibrothal Furnace Muffle
6. Insulating Brick
7. Pulley Wire
8. Kaowool

**Table 2.2: Molten Salt Median Viscosity Cup Drain Time, seconds**

| | | Orifice Size | |
|---|---|---|---|
| **Material** | **Temp.** | **No. 1** | **No. 3** |
| $Na_2CO_3$ | 880°C | 25.2 | -- |
| $Na_2CO_3$ | 950°C | 26.2 | 13.0* |
| $Na_2CO_3$ with 10 wt% $SiO_2$ | 950°C | 28.2 | |
| $Na_2CO_3$ with 15 wt% $SiO_2$ | 950°C | 29.6 | |

*Times less than 20 seconds are not considered reliable.

Using this equation, at 880°C the viscosity of pure sodium carbonate is 3.83 cp; the viscosity at 950°C is 3.23 cp. Our results showed a slight increase in the viscosity of molten sodium carbonate as the temperature was increased, although this increase is probably not significant given the relative error (nominally ± 0.5 s) for each measurement.

Once ash surrogates were added to the melt, a variety of difficulties were encountered. We were unable to collect acceptable data at 880°C, since insufficient wetting occurred. We were only able to obtain acceptable data with silica loadings of 15 wt% or less. With a silica loading of 20 wt%, the dip cup having the largest orifice, cup number 5, would not fill with melt. When alumina was added, 10 wt% produced very inconsistent flow times with the melt behaving as though it contained lumps. A 20 wt% alumina mixture had the consistency of a paste. Adding 10 wt% of kyanite produced a viscous mixture that would not fill the dip cup while 20 wt% made a mixture that was dry in appearance.

Numerous melts were attempted in smaller 50 mL alumina crucibles to examine the higher viscosity specimens. In one such test, the silica was observed to settle to the bottom of the melt. It is not known whether this happened in any of the viscosity tests, although the relative consistencies of the measured flow times makes this unlikely. No flow measurements were made with the surrogate ash materials at the 30 or 40 wt% level. One additional 50 mL melt was made, adding 20 wt% silica to a blend of 80% sodium carbonate and 20% sodium chloride. When melted, the salts became fluid but the silica formed a skeletal structure that never settled into the melt.

Given the ash surrogates that we used, the molten sodium carbonate, in an air atmosphere, could not accept a silica content greater than 15 wt%, or alumina or kyanite loadings as high as 10 wt%. Since the rheological behavior of the melt is highly sensitive to the morphology (particle size and surface area) of the ash, different choices for the alumina, silica, and kyanite would have yielded different results. Suspension of the ash surrogates was also a problem, as evidenced in some of the higher $SiO_2$-loaded 50 mL mixtures. Given the comparable densities of silica (in the range of 2.3–2.6 $g/cm^3$) and molten sodium carbonate at 950°C (1.93 $g/cm^3$),[4] this difficulty is not completely unexpected. Keeping these mixtures suspended while conducting any type of viscosity measurement will present a real problem.

Also, when the salt and an ash material are blended together as powders before melting, as was done here, the resulting melt may not simulate the behavior that would be seen if the salt was melted first and the ash added later.

Without the presence of $CO_2$, which is formed during the normal oxidation process in the MSO reactor, sodium carbonate will decompose to form sodium oxide and $CO_2$ beginning at about 500°C. Under the given test conditions, weight losses of up to 10% were observed in 7.5 hours. Because of this change in melt composition, no measurements were made on the effect of time (greater than 8 hours) on melt viscosity. Had the experimental apparatus had the capability to provide a partial atmosphere of carbon dioxide, this weight loss/change in melt composition would have been avoided and longer term experiments could have been run.

Performance Metric

LLNL will perform experiments to determine salt viscosity as a function of ash composition, ash concentration, temperature, and time. These experiments will also discern whether or not there is a critical ash loading above which the salt will freeze in the vessel and not be readily removable by remelting. These experiments will enable us to establish a salt recycle schedule for MWMF based upon ash content, and provide information pertinent to heater design, in the event of emergency shut-down, to remelt ash-bearing salt. Attainment of this goal will constitute success for this technical issue.

Results

The dip cup viscosity technique chosen for this work is simple and inexpensive, and yielded good results with salts of low viscosity. Because of the unexpectedly viscous nature of many of the salt compositions specified for this subtask, the test method did not perform to our satisfaction. Further work is suggested, in which the experimental procedure would be modified as follows. First, detailed analysis of real ash should be done to fully characterize the particle size distribution and surface area to enable better surrogates to be chosen. A viscometer of the rotating spindle type should be used, requiring the fabrication of platinum spindles, since the standard Brookfield set-up cannot be used at the temperatures specified herein. Lastly, the apparatus should have the capability to provide a partial $CO_2$ atmosphere, with the salt composition monitored via DTA-TGA, to eliminate $CO_2$ loss from decomposition.

## 3. Sodium Carbonate Volatility

Task Objective

The volatility of sodium carbonate and sodium chloride under static conditions is well known. High throughputs of waste and oxidant air in the MSO process will affect the amount of sodium carbonate that exits the reactor. Experiments will be conducted to gain a quantitative understanding of the amount of sodium carbonate entrained in the off-gas as a function of gas velocity through the melt and chloride content in the melt.

Experimental Methodology and Results

Carryover of salt is obtained via two mechanisms. First, the vapor pressure of sodium carbonate and sodium chloride is significant at temperatures between 900–100°C. As the other non-condensable gases exit the reactor, salt vapor will therefore also exit the reactor in quantities proportional to the vapor pressures of the other gases ($CO_2$, $O_2$, $N_2$, Ar, etc.). Experience at ETEC has shown that vapor carryover of ~ 0.7 mg of sodium carbonate can be expected per liter of gas at nominal operating temperatures of 900°C.[5] Calculations show that at similar temperatures vapor carryover for pure sodium chloride will be on the order of 3 mg/L.[6] Therefore, vapor carryover should increase with the addition of NaCl to the melt at these temperatures. Second, some amount of salt will exit the reactor as a "mist," depending upon the turbulence in the reactor bed and the convolution of the path relative to the line-of-sight of the exhaust gas outlet.

Non-insulated, modular straight pipe sections were designed and installed in the off-gas line. The lack of insulation aided the condensation of the salt vapor in these pipe sections. We measured the quantity of salt deposited in a steel wool filter inserted into the off-gas pipe, and also examined qualitatively how well the salt adheres to the pipe walls after condensation. All sections were weighed daily and carryover recorded. All tests have been done with no baffles in the MSO reactor, so that an absolute amount of carryover could be determined.

Carryover was measured for all experiments run using the coaxial injector for the Carbon Monoxide Emissions subtask, with an average superficial velocity of 1 ft./s. Table 3.1 shows the amount of salt accumulation seen as a function of sodium chloride content; this information is shown graphically in Figure 3.1. Data previously reported in the interim summary for pure sodium carbonate using the cooling injector indicated an average deposition rate of approximately 2.33 g sodium carbonate per hour. A rate approximately double that was seen with the new injector, which we believe is due to higher turbulence in the melt achieved with the coaxial injector.

**Table 3.1: Salt Carryover With No Baffles and Coaxial Injector**

| mol% NaCl | Avg. Loss (g/hr) |
|---|---|
| 0 | 5.36 |
| 10 | 6.52 |
| 20 | 8.94 |
| 30 | 17.92 |

The amount of carryover increased by a factor of 3.3 with the addition of up to 30 mol% sodium chloride. An increase in carryover was expected based on the increased vapor pressure of NaCl, but the increase can also be partially attributed to the decrease in surface tension with the addition of NaCl. The surface tension of

**Figure 3.1: Salt Carryover as a Function of NaCl Content**

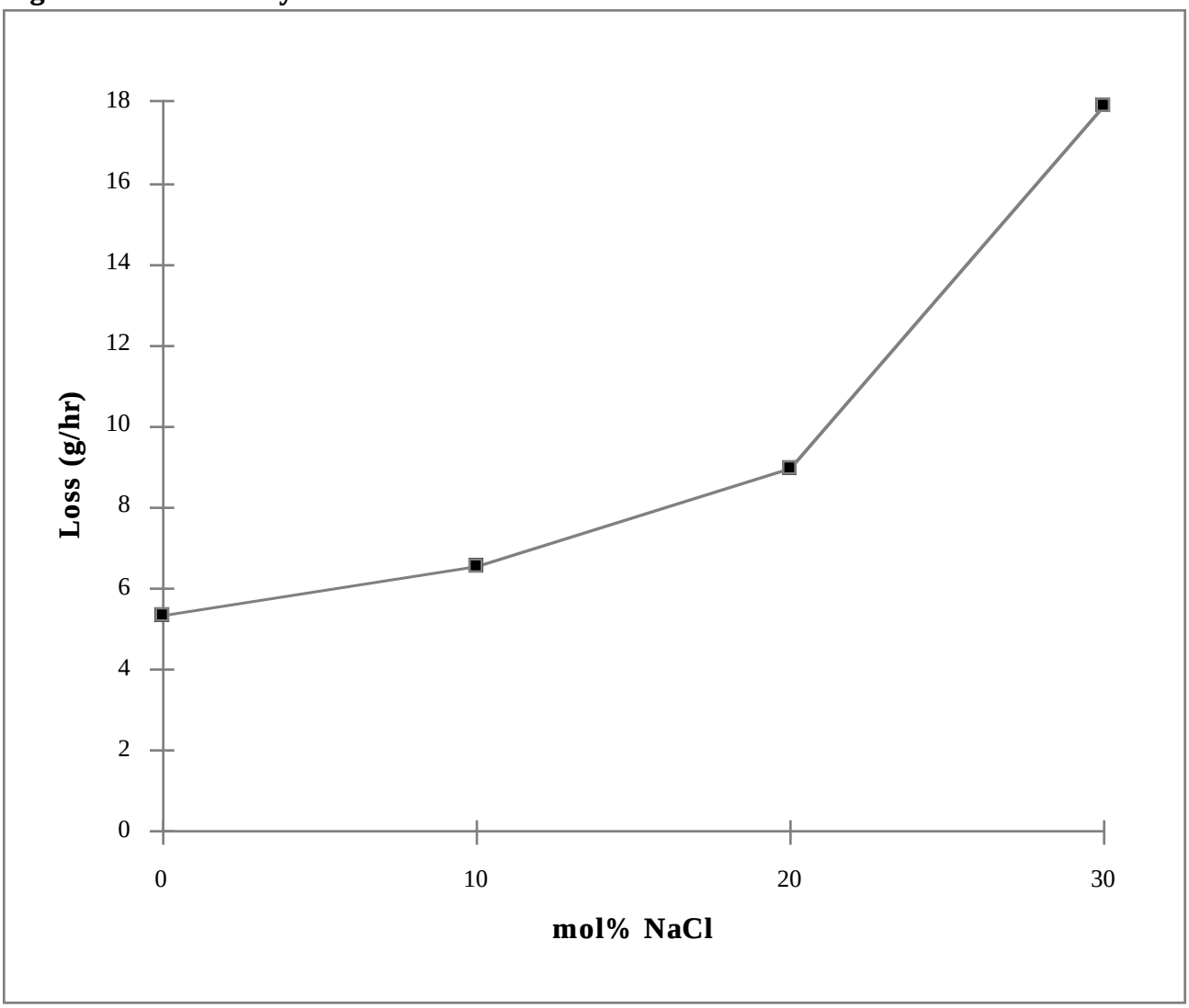


NaCl is approximately half that of $Na_2CO_3$ (at 950°C, the surface tension is 103 dyn/cm for NaCl and 207 dyn/cm for $Na_2CO_3$).[7] The NaCl appeared to act as a surfactant in the sodium carbonate melt, increasing the amount of frothing seen in the reactor as the concentration of NaCl was increased. The foaming resulted in smaller diameter particles, with subsequently higher terminal velocities, which had a much higher probability of exiting the reactor with the off-gas without baffles to block the line of sight of the gas outlet.

We also examined the carryover as a function of superficial velocity through the reactor by running ethylene glycol and toluene through the MSO reactor with a pure sodium carbonate melt. Carryover observed, in terms of both grams of sodium carbonate per hour and milligrams of sodium carbonate per liter, is compiled in Table 3.2 for superficial velocities of 0.5, 1.0, 1.5, and 2.0 ft./s. As $V_S$ was increased by a factor of four, the amount of salt deposition observed (g/hr) increased by a factor of three during the toluene experiments, although the increase was fairly small on a

per liter basis. Much higher carryover was seen during the ethylene glycol experiments. This higher carryover on a per liter basis appears to correspond to the higher amount of water generated during the oxidation process. (The theoretical amounts of water in the off-gas for a 1.0 ft./s run with 120% excess air are 7.9 vol% for toluene and 17.9 vol% for ethylene glycol.) We do not as yet have any theories that would explain this observation.

**Table 3.2: Salt Carryover as a Function of $V_s$**

| $V_s$ (ft./s) | Toluene | | | Ethylene Glycol | | |
|---|---|---|---|---|---|---|
| | Air Flow (SLPH) | Avg. Loss (g/hr) | Avg. Loss (mg/L) | Air Flow (SLPH) | Avg. Loss (g/hr) | Avg. Loss (mg/L) |
| 0.5 | 1816 | 2.40 | 1.32 | 1582 | 2.70 | 1.70 |
| 1.0 | 3631 | 2.19 | 0.60 | 3164 | 13.4 | 4.24 |
| 1.5 | 5434 | 4.07 | 0.75 | 4746 | 50.1 | 10.6 |
| 2.0 | 7238 | 6.11 | 0.84 | 6328 | 53.5 | 8.45 |

In qualitative examinations done daily, it was noted that a very thin (< 1 mm) layer of salt uniformly deposited on the outlet stub (located immediately at the exit to the reactor, just prior to entering the modular section of pipe) during normal operations. This coating easily came off when a gloved finger was rubbed over it; a bottle brush or similar cleaner can be used to clean pipe walls.

Performance Metric

Success for this task would be the determination that the amount of sodium carbonate entrained in the off-gas is minimal, and that any deposited salt can easily be removed from the piping using a soot blower or other means. A minimum result is assurance that MSO pilot plant operation is practical ($10^2$ to $10^3$ hours). A preferred result is that an MSO pilot plant can operate for practical periods ($10^3$ to $10^4$ hours) without shutdowns for cleanout.

Results

The amount of carryover has been measured, and has been found to increase with the amount of sodium chloride present and the superficial velocity. The amount of carryover can be mitigated via the use of baffles. First, the baffles will form a tortuous path for the exhaust gas to follow, which will deter particles from following a simple line-of-sight to the exhaust exit. Second, baffles located in the upper portion of the reactor can be designed as a heat sink, minimizing the vapor carryover as well. ETEC has successfully demonstrated the effectiveness of baffles; work will soon be underway to design and demonstrate baffles for the MWMF MSO system. The salt which was entrained in the off-gas and deposited in pipe sections with steel wool filters was easily removed, indicating that the use of a soot blower will easily remove any carryover from the exhaust pipes. By utilizing baffles and periodically operating a soot blower, MSO pilot plant operation for periods on the order of $10^3$ hours without shutdowns for cleanout of off-gas pipes should be practical.

## 4. Final Forms

Task Objective

The objective of this task is to demonstrate and evaluate a waste form—polyethylene microencapsulation—for land disposal of salt residues from the MSO process. The technology is judged against leach (TCLP) behavior, mechanical durability and production practicality.

Methodology

The waste form investigated is MSO salt microencapsulated in low-density polyethylene (LDPE). Typically, the waste form is fabricated as a large monolith by extruding a mixture of salt and molten polyethylene into a 55-gal drum. Experiments were designed to elucidate effects of waste characteristics and process parameters on performance. Of particular interest are practical loading levels and how the particle size of the salt influences leaching at high loadings. Chemical modification of the MSO salt to minimize leaching of its hazardous constituents was not part of this study. The study was guided by a literature survey, theoretical considerations, prior experience, and results of other current projects. The literature survey was not intended as a critical review, and no attempt was made to rationalize the diverse and complicated phenomena that have been reported.

Waste form specimen fabrication, characterization and leach testing were carried out by EG&G Rocky Flats under an Integrated Contractor Order (Andrea M. Faucette, P.I.). Some salt preparation and specimen characterization was done at LLNL. Fabrication was by twin-screw extrusion. Specimens were prepared in the form of chopped rods and small monoliths.

Salts selected and prepared were residual $Na_2CO_3$–NaCl salt (0, 10, 20, 30 mol% NaCl) from LLNL MSO experiments on surrogate wastes and six varieties of food grade NaCl representing two particle morphologies and a several particle size ranges. The MSO salt was untreated except for comminution and drying.

Waste form characterization and evaluation included chemical analysis, microscopy and leach testing. Strength was judged qualitatively, but mechanical properties were not measured. Leach resistance of MSO demonstration specimens employed the TCLP test. Weight loss upon extended leaching in water was also measured.

Some technical details (concerning, for example, equipment configurations and chemical analysis techniques) are omitted from this report. These will be documented in various LLNL and EG&G internal reports and memoranda.[8,9] Some of the leach test results were unavailable for this report; they will be documented likewise.

Task Variances

The work accomplished deviates from the Technical Work Plan in several ways. These deviations occurred because of time shortages. Delays were occasioned by procurement difficulties, a mislaid shipment, and the inadvertent inclusion of used MSO salt containing $K_2CO_3$. The variances are as follows:

1. Some work in progress is unfinished at this time. This includes analytical results of some leach tests, chemical analyses to confirm some results, additional microscopy, and theoretical calculations. The work will be completed shortly and documented as noted above.

2. It had been intended that the MSO salt encapsulated would be "filtered salt" (see below). "Used salt" was substituted. However, portions of each salt batch provided to Rocky Flats were retained by LLNL. These are being converted to filtered salt and will be microencapsulated under other funding. The used salt employed in the present experiments is a more severe test of the waste form.

3. The NaCl was a surrogate for "separated salt." The TWP had called for additions of $Na_2CO_3$ to simulate the probable incomplete separation that would in practice be typical. This was not done.

4. No experiments of synthetic MSO salt ($Na_2CO_3$–NaCl) spiked with RCRA metals or radionuclide surrogates were done.

Background

Molten salt oxidation of mixed waste containing chlorinated hydrocarbons results in the formation of NaCl and ash (inorganic oxides, free metals, etc.). The concentration of organic compounds is negligible. Disposition of used salt without further treatment would generate excessive volumes of waste. An MSO treatment train would most likely separate the NaCl and/or ash for disposal, and recycle the $Na_2CO_3$. The ash might be immobilized as a ceramic or glass waste form.

Thus, MSO residual salts can be grouped into three general types. By *used salt* we mean residual MSO reactor salt ($Na_2CO_3$ contaminated with NaCl and various inorganic compounds) that has not been treated, except possibly comminuted. (To *comminute* is to reduce a material to a powder or to reduce its particle size, as by ball milling.) *Filtered salt* is used MSO salt that has been dissolved in water, filtered to remove low-solubility inorganic compounds, and dried—but separation of $Na_2CO_3$ and NaCl is not done. In *separated salt*, most of the $Na_2CO_3$ is removed prior to drying.

Polyethylene microencapsulation for immobilizing waste salts is a fairly well-developed technology which provides a durable waste form with good salt loadings at reasonable costs. Advantages include the use of standard polymer processing technology, insensitivity to waste chemistry, excellent matrix stability,[10,11] minimal processing and storage hazards to personnel and the environment,[12] the ability to use recycled LDPE, the option of reprocessing an unsatisfactory product, and general appeal to non-technical stakeholders. Leach resistance is generally satisfactory, though its dependence on loading levels, salt characteristics and processing parameters is complicated and far from being completely understood. The waste form itself is quite robust, and the polyethylene itself is very resistant to degradation.[10,13] Equipment costs are somewhat high relative to competing technologies.

As with any waste form technology, the "performance" of LDPE microencapsulation depends on how it is tested. A crushed monolithic form may leach more than extruded pellets. (In the latter case, the surface polyethylene tends to smear over the

salt grains; in the former, salt is simply exposed on fracture surfaces.) It can argued that the monolith is so rugged that leach testing only after being broken up is an unduly severe requirement. Some organizations are seeking regulatory relief on this matter, but the TCLP test is presently the basic requirement.

The general theoretical picture entertained by workers in this field is that at relatively low loadings, significant leaching occurs only from salt particles exposed at the surface of the waste form. Diffusion of contaminants through the LDPE itself is thought slight. As loadings increase, there is an increasing probability of mutual contact between salt grains, resulting ultimately in interconnected salt clusters throughout the waste form. At these excessive loadings, virtually none of the salt is isolated from the environment, and leach resistance degrades catastrophically. Obviously, this implies that performance is dictated by volume fraction of loading rather than weight fraction, both mechanistically and in the volume of final waste form generated. Particle size, according to this picture, should have an important impact on leach resistance. If the particles are largely isolated from one another, leaching should dissolve the salt only to an average depth on the order of the mean particle size. Quantitatively, the total amount leached (for the same loadings and specimen geometry) should scale proportional to the mean particle size.[8]

Therefore, two prime considerations in process development are the ability to encapsulate fine-grained salt, and keeping the salt particles separated. In this regard, twin-screw extrusion provides significant technical advantages over single-screw extrusion, because the higher shear rates of the former provide more intimate mixing and dispersion of the salt in the LDPE. In general, a twin-screw extruder tolerates a broader range of salt properties (size, morphology, fluffiness, free-flowing) than a single-screw one. A fairly obvious concept is to add a surfactant, such as a stearate, to the extruder feed. This should inhibit agglomeration. Unfortunately, stearates also lubricates the melt in the extruder, and experiments with a single-screw extruder[14] showed that extruder output decreased to unacceptable levels. This effect may be less severe in a twin-screw extruder.

Preparation of the salt prior to extrusion is also important. In particular, the method of drying a filtered brine strongly affects the salt morphology.[15] In small-scale laboratory studies, brines are typically dried in an ordinary oven and then ball milled. Salt prepared by certain commercial-scale drying and comminution methods might differ significantly from the laboratory salt.

Leaching of metals accompanying the salt is far more complex, involving the chemistry and physical condition of the waste. A good example is the present TCLP results given below. This topic is too lengthy to discuss in detail here, and the reader is referred the literature.[16] Chemical modification of the waste (“conditioning,” “stabilizing”) prior to extrusion seeks to exploit the complexity to minimize leaching of the hazardous components. In general, there has been little in the way of studies focusing on the detailed mechanisms of leaching. Phenomenologically, leaching follows a diffusion law,[17] but the actual mechanisms remain obscure and probably operate simultaneously in complicated ways.

Experimental studies of salt microencapsulation have mainly involved nitrates; carbonates and chlorides have received less attention.[18] Relatively little has been reported on the microencapsulation of actual MSO salt waste. The potential efficacy of LDPE microencapsulation was demonstrated at BNL on residual salt from Rockwell MSO experiments.[17] The only RCRA metal present in significant amounts was chromium at 3000 ppm. The salt was microencapsulated using a single screw extruder at 50 wt % salt. TCLP leachate concentration of chromium was only 1 ppm.

Experimental Methods and Results

*Materials*

Six varieties of NaCl were procured from Morton Salt Company. These encompassed two particle morphologies and several particle size ranges. All were food grade, contained anticaking agents and were not iodized. Their nominal properties according to the manufacturer are given in Table 4.1. As discussed below, scanning electron microscopy (SEM) confirmed the general characteristics.

**Table 4.1: Characteristics of NaCl**

| Morton commodity code* | Morton name | Anticaking agent* | Mean particle size (μm) | Crystal form |
|---|---|---|---|---|
| 1312 | TFC 999 Salt | $Na_4Fe(CN)_6$ | 460 | cubes |
| 1328 | TFC 999 Fine Salt | $Na_4Fe(CN)_6$ | 290 | cubes |
| 1226 | 50/50 Flour Prepared Salt | $Ca_3(PO_4)_2$ | 200 | cubes |
| 1255 | Pulverized Salt, Extra Fine 200 | $Ca_3(PO_4)_2$ | 35 | jagged fragments of cubes |
| 1247 | Pulverized Salt, Extra Fine 325 | $Ca_3(PO_4)$ | 25 | *ditto* |
| 1482 | Flour Salt | $Na_4Fe(CN)_6$ & $Ca_3(PO_4)_2$ | 120 | *ditto* |

* Concentrations ~1-2 wt% $Ca_3(PO4)_2$, ~5 ppm $Na_4Fe(CN)_6$

The residual MSO salt was obtained from the LLNL MSO reactor used in other tasks of this study. The salt had been used to treat surrogate liquid waste, including both halogenated and non-halogenated hydrocarbons. Neither the salt nor the hydrocarbons were spiked with metals. The principal contaminant in the salt was chromium from corrosion of the stainless steel reactor. The first batch of salt sent to Rocky Flats had not been specially prepared for this experiment but was an accumulation of salts from a wide variety of run conditions. Chunks of salt were retrieved from this material. Workers at Rocky Flats in turn segregated this material into two groups according to their quite different color. These are here referred to as “gray” and “green” MSO salt. Analysis confirmed that the green salt, as expected from its color, contained high levels of Cr; the gray salt did not. Subsequent to encapsulation it was discovered that the gray salt was in fact a ternary

mixture of lithium, sodium and potassium carbonates used in earlier MSO experiments. The results on the gray salt are included here. Four other batches of residual salt from the same reactor, again contaminated by corrosion, were retained specifically for the encapsulation studies. These were mixed salts—$Na_2CO_3$ containing (0, 10, 20 & 30) mol% NaCl.

The LDPE used was "Chevron 1409 LDPE," which has a density of 0.92 g/cc and a melt index (MFI) of 50.

*Specimen fabrication*

The MSO salts were size-reduced in a jaw crusher, dried in an oven overnight to remove any residual moisture, and then ball-milled to a uniform size suitable for extrusion. The milled salt was examined by SEM. The particle size ranges from ~25 μm down to sub-micrometer size. The smaller particles appear to be somewhat agglomerated. Six 50-lb bags of the NaCl described above were evaluated and, as mentioned, was found consistent with the properties in Table 4.1. These salts required no pretreatment or special handling prior to extrusion. Thus, a total of twelve salt types (six MSO residuals and six commercial NaCl) were used.

The twin-screw extruder (Berstorff model ZE 25) has seven barrel sections, a bore diameter of 25 mm, and a length:diameter ratio of 34. The screw configuration used was a "strong" configuration, meaning that a considerable amount of work was imparted to the polymer/salt mix as it moved through the extruder barrel.

Initially, a K-Tron side stuffer feeder was used to convey the material into the melt stream via a side port. Several samples were collected using this configuration. However, the side-stuffer feeder had difficulties keeping up with the loss-in-weight feeder, resulting in reduced throughput rates and inaccurate waste feed. Discussions with the manufacturer indicated that the screws in the side-stuffer feed were not optimal for the waste feed. Improved screws were unavailable until late January. In the interim, the extruder was reconfigured so that the waste could be fed into the throat of the extruder using a small volumetric feeder (Accurate 100). The main limitation of this arrangement was the limited throughput of the small feeder and the fact that the only practical way to vary the waste loading was to vary the rate of the LDPE while feeding the waste at a constant rate. Unfortunately, this resulted in a varied overall throughput. The constant throughput originally intended provides more constant process conditions—filling of the screw flights, shearing forces, etc. However, as discussed later, much more accurate waste loadings were obtained.

On 1/11/95, the MSO gray salts were re-run using the new configuration. The Morton commodity code 1482 NaCl salt, designated FS-120, was also run on this date. The remaining salts were not received until 1/18/95, and these were run on 1/19/95. Run sheets for all extrusion operations are available.[8,9] High melt temperatures (> 200°C) were observed. Compared with the set points (170°C), this indicates that the extruder screw configuration is stronger than required for this material. Replacing the dispersive mixing elements (kneading block) with distributive mixing elements (pin mixers) should decrease the melt temperature

and increase the throughput rate. This may also alleviate some of the side-feeder problems noted earlier.

Loading levels are presented on a mass basis. As noted in the previous section, the waste form is more easily understood when interpreted in terms of volumetric loadings. The following table gives the comparison for the two salts used:

**Table 4.2: Weight and volume fractions for NaCl and $Na_2CO_3$**

| wt% salt | vol% NaCl | vol% $Na_2CO_3$ |
|---|---|---|
| 30 | 15.4 | 13.5 |
| 40 | 22.1 | 19.5 |
| 50 | 29.8 | 26.7 |
| 60 | 38.9 | 35.3 |
| 70 | 49.8 | 45.9 |

Initial nominal loadings were 40, 50, 60 and 70 wt% salt. At 70 wt%, however, the waste form was visually judged unsatisfactory, and no more was made. Waste form was extruded using the twelve salt types, each at loadings of 40, 50 and 60 wt%.

The waste form was extruded as strands ~7 mm diameter. The extruded strands were chopped with a paper cutter to form short rods. Thus, though there was some smearing of the LDPE on the cylindrical surfaces, the encapsulated salt was exposed on the ends. Small monoliths were made by collecting the extrudate in 250-mL polypropylene beakers. At 60 wt% loadings, the extrudate was too stiff to flow well in the beakers, so these are somewhat irregular in appearance.

*Specimen characterization*

Deviations of waste loading from the set point can be caused by inaccuracies in the feeders and surging in the extruder. Most of the deviations in the present experiments are probably due to problems with the waste feeder. (Surging is less common the twin-screw than in single-screw extruders.) The actual waste loadings were determined by a thermal ashing technique,[8,9] in which the LDPE is decomposed at 600°C. Verification tests have indicated that the method is accurate to within ±2% for the materials used here. Ashing results are presented in Table 4.3. Only data from MSO-gray and FS-120 salts are available. Each data point is the average of four replicate experiments. MSO-gray data marked 1/9/95 are from samples run using the side-stuffer feeder, while that marked 1/11/95 is from samples using the volumetric feeder.

The ashing results confirm that feeding the salts into the throat of the extruder is more accurate results than feeding through the side stuffer. This is contrary to what is normally observed in extruder compounding operations. As previously mentioned, this would probably be corrected by replacing the sub-optimal screws.

SEM analysis was performed on unencapsulated and encapsulated MSO salts and FS-120 salt. All specimens were prepared by the cold fracture method, in which the specimen is immersed in liquid nitrogen prior to fracturing it. Representative

**Table 4.3: Ashing and immersion test results.**

| Salt type | Sample no. | Nominal loading wt% | Loading by ashing wt% [σ] | | Weight per cent of salt lost | |
|---|---|---|---|---|---|---|
| | | | 1/9/95 | 1/11/95 | 1/9/95 | 1/11/95 |
| MSO gray | 1a | 50 | 59.6 [1.4] | 50.2 [1.6] | 12.3 | 14.6 |
| | 1b | 50 | | | 12.5 | 14.8 |
| | 1c | 50 | | | 11.7 | 13.9 |
| | 2a | 60 | 67.7 [0.61] | 63.4 [0.56] | 63.6 | 67.9 |
| | 2b | 60 | | | 65.9 | 70.3 |
| | 2c | 60 | | | 53.5 | 57.1 |
| | 3a | 70 | 65.3 | | 51.7 | |
| | 3b | 70 | | | 65.4 | |
| | 3c | 70 | | | 68.1 | |
| FS-120 | 4a | 50 | | 50.6 [0.46] | | 7.9 |
| | 4b | 50 | | | | 7.7 |
| | 4c | 50 | | | | 7.6 |
| | 5a | 60 | | 60.8 [0.22] | | 16.1 |
| | 5b | 60 | | | | 17.2 |
| | 5c | 60 | | | | 17.4 |
| | 6a | 70 | | 70.7 [0.26] | | 46.5 |
| | 6b | 70 | | | | 45.2 |
| | 6c | 70 | | | | 47.3 |

micrographs of encapsulated salts are shown in Figures 4.1 & 4.2. (See also refs. 8 & 9.) Some general observations are as follows. It should first be noted that salt grains can be pulled out during specimen fracture, so the micrographs may not reveal the full concentration of salt present. Previous SEM analyses at Rocky flats of extruded nitrate salts identified substantial agglomeration of the waste material within the LDPE matrix. This does not seem to be occurring with the LLNL MSO salts (*cf.* Figure 4.1). Also, in comparing the encapsulated with the unencapsulated MSO salts, there does not appear to be any evidence of secondary agglomeration in the extrusion process. Indeed, Figure 4.1 shows little sign of agglomeration after extrusion. This may reflect the very strong extruder conditions. Very small and bright spots were seen in the MSO specimens at high magnifications (~2000×). These are concentrations of heavy elements, probably chromium compounds. There is there is no gross evidence of any change in the particle-size distributions upon encapsulation of either the MSO or FS-120 salts. Some micrographs show round "craters." These are caused either by air entrainment or possibly moisture in the salt which vaporized to steam in the process. (Voids left behind when salt grains are pulled out during specimen preparation have a different appearance.) This is indicative of a possible need to use a vacuum port during extrusion. Naturally, the

**Figure 4.1: LDPE-microencapsulated MSO-gray salt, 60 wt% loading.**

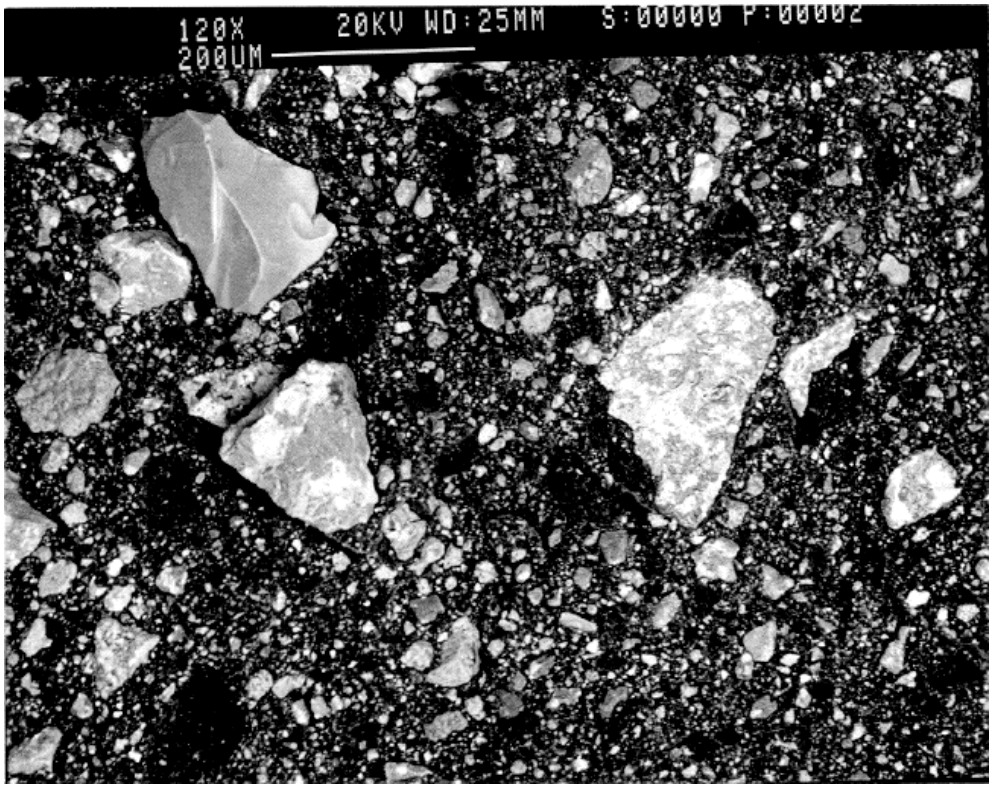


**Figure 4.2: LDPE-microencapsulated FS-120 salt (NaCl), 70 wt% loading.**

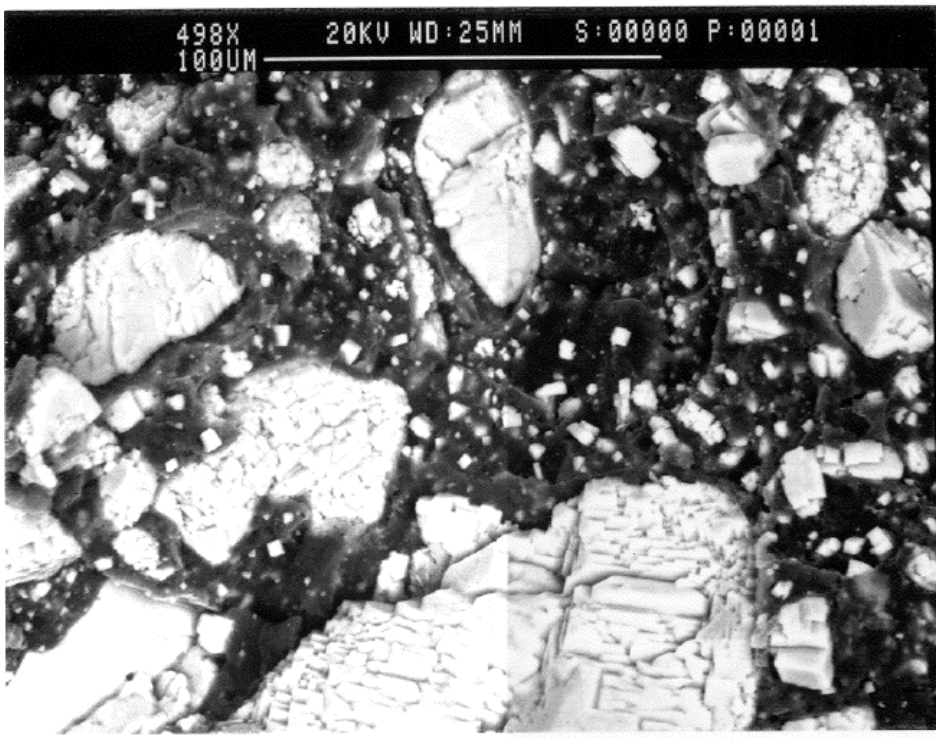

bright spots seen the MSO salts were not in the FS-120, which contained no heavy elements.

MSO-gray salt at 40 and 60 wt% loadings were examined by optical microscopy at LLNL. The specimens were removed from monoliths, mounted in epoxy in the standard metallographic manner, and polished to a 1-μm finish. Moisture caused rapid deterioration of the exposed salt, and further work is planned. One has, however, the immediate impression that salt in the 60 wt% material is far more interconnected than in the 40 wt% one, and also that it is more concentrated and interconnected than one would suppose from SEM images (Figure 4.1).

*Strength*

The mechanical properties of the waste form were not measured quantitatively. The MSO-gray waste form at 40 wt% loading was, however, quite robust. It requires a considerable blow from a steel hammer to break it. (Test specimens are usually broken off with a hammer and chisel.)

*Immersion tests*

The degree of encapsulation was assessed using an immersion dissolution test. Testing was performed on two sets of two samples for each waste form. Samples were strands of length 1.50 ± 0.25 in (38.1 ± 0.64 mm), and diameter ~ 7 mm, with broken surfaces on both ends. Two strands were dried and weighed after immersion for two days, and two strands after five days. The test was designed to reveal the maximum leaching. (Unlike the metal contaminants, the salts themselves are highly soluble in water). It provides a semi-quantitative comparison of the degree of encapsulation between samples prepared using different extrusion parameters or salts having differing physical properties. At this time, only the results for the MSO gray and green salts, and for the FS-120 NaCl are available. The results are given in Table 4.3 above.

The severe increase in MSO-gray leaching observed between the 50 and 60 wt% levels suggests that particle interconnection had become widespread. The corresponding jump for FS-120 salt occurs at a higher loading, between the 60 and 70 wt% levels, though there is also a significant increase between 50 and 60 wt%. In addition to the location of these leaching increases, the overall leaching of the NaCl appears to be significantly less than that of the MSO-gray. On the basis of the data in Table 4.3, however, it is not clear whether this is true on a volumetric loading basis—the main jump occurs in the 39-50 vol% range for NaCl. Unfortunately, the only MSO salt data available at this time is for the MSO-gray specimens, for which the volumetric loading could not be determined—because the density of the (Li-Na-K)$_2$CO$_3$ mixture (see *Materials*, above) is unknown.

Visual examination of the leached the specimens provides additional information. Figure 4.3 is a photomacrograph of three MSO-gray specimens after immersion testing. The depth of leaching is seen to progress with increasing loading levels. (This is hard to see in Figure 4.3 for the 50 wt%, but is evident in the original photograph). Moreover, the *extent* of leaching within this rind (as we term it) seems greater for the 70 wt% specimen than in the 60 wt% one. Note that the cores of all three specimens have the same appearance. The straightforward explanation

**Figure 4.3: LDPE-microencapsulated MSO-gray salt waste form after immersion testing. 50, 60 & 70 wt % waste loading, left to right. Diameters are on the order of 7 mm. Note the salt-depleted "rind" (see text).**

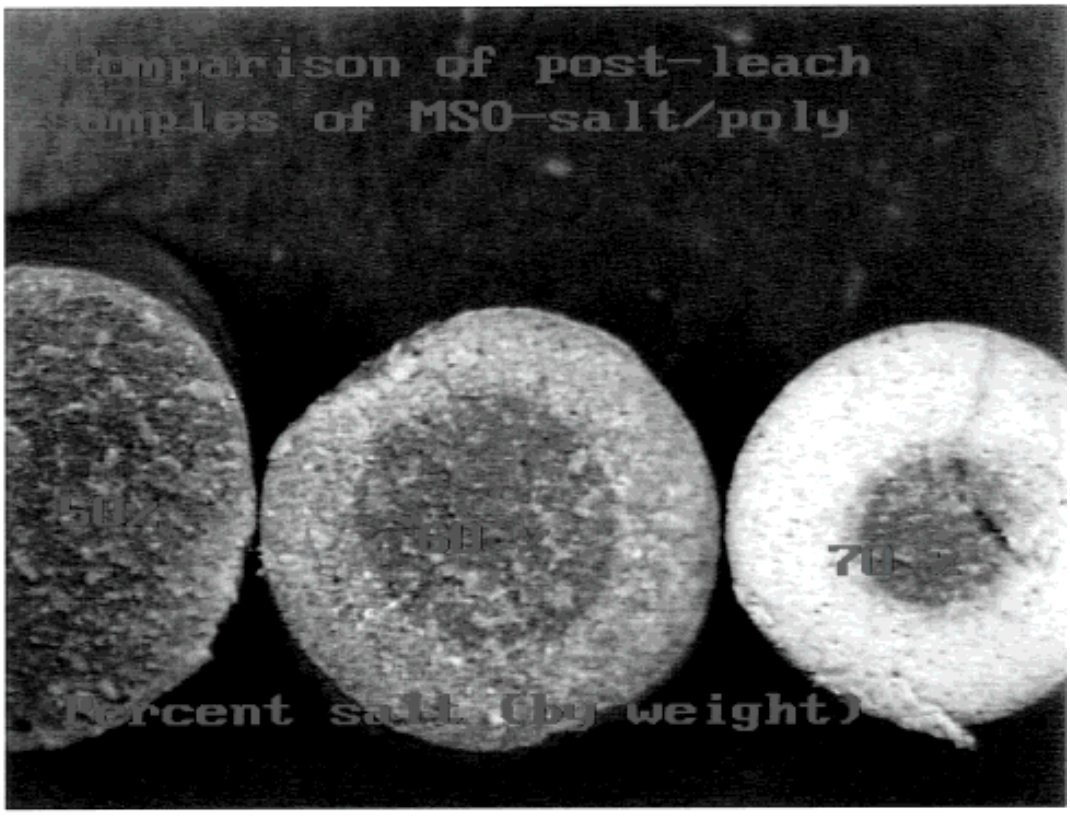


is that at 50 wt% the salt grains are not much interconnected; at 70 wt% they are highly interconnected; and at 60 wt% there are interconnections throughout the material, but much less of the salt is continuously connected to the surface. (This is just the sort of behavior one would expect from a percolation theory model.)

The corresponding photograph for the FS-120 specimens is not included but shows a qualitatively similar sequence. Quantitatively, however, the thicknesses of the rinds at 60 and 70 wt% are about half that of the corresponding MSO-gray specimens and were not observable (on this scale) in the 50 wt% FS-120 specimen. There is evidently a difference in the *rates* of leaching for the two salts as well as in the extent of leaching.

*TCLP Tests*

TCLP analyses were run on six unencapsulated MSO salt samples and seven MSO salt samples encapsulated at various waste loadings. For the unencapsulated salts, triplicate samples of the gray and the green sub-populations were tested. The salt chunks were crushed in a Bico jaw crusher with the jaw spacing set at 3/8 in (~9.5 mm). The triplicate samples were taken from homogenized batch samples in order to estimate the data variability due to laboratory analysis as compared to extrusion or sampling operations. The encapsulated samples were collected initially as strands and then cut to <9.5 mm lengths with a paper cutter. Because of the limited amount of sample available, duplicates were not run on the MSO-green salt.

The TCLP results are summarized in Table 4.4. The unencapsulated samples were below detection limits of Ag, Cd and Ni but significantly above the treatment standard for Cr. The green samples showed particularly high Cr leach rates. The final pH of the extract was approximately 9, which is near the minimum solubility point for Cr. Nonetheless, Cr concentrations were as high as 300 ppm. This suggests that the total Cr content in the salt is >1000 ppm. This was expected both because of the color of the salt and because corrosion of the LLNL reactor vessel had been observed.

The encapsulated samples also exceed the treatment standard for Cr. This is largely due to the way the TCLP is conducted. Depending on the buffering capacity of the material being evaluated, an extraction fluid with a pH of either 4.93 or 2.88 is used. The choice of the which fluid to use is determined from a 5-g subsample size-reduced to <1 mm. Because of the high buffering capacity of the salts, the more acidic extraction fluid was used. During the extraction phase of the TCLP, the unencapsulated salts raised the pH of the extraction fluid to a final value of approximately 9. At this pH, heavy metals such as Cr are relatively insoluble and are typically filtered out of solution. When the salts are encapsulated, however, the pH remains lower, and the heavy metals that do leach into the extraction solution are more soluble.

This effect can be seen in the LDPE-encapsulated MSO salts. Better encapsulated samples (lower waste loadings) leached much less metal ions into the extraction solution. However, since the final extract pH was lower, the heavy metals that leached into the solution were more soluble.

There is at present some concern that there might have been some interferences occurring the TCLP atomic absorption analyses. They are therefore being confirmed by atomic emission spectroscopy, but results are not yet available.

**Table 4.4: TCLP leach test results.**

| Green salt | | | Gray salt | | |
|---|---|---|---|---|---|
| **wt % salt (nominal)** | **Cr (ppm)** | **Final pH** | **wt % salt (nominal)** | **Cr (ppm)** | **Final pH** |
| 40 | 9.84 | 4.08 | 50 | 5.87 | 5.92 |
| 50 | 22.4 | 4.57 | 50 | 7.99 | 6.88 |
| 60 | 60.7 | 6.44 | 60 | 12.2 | 8.23 |
| 100 | 254 | 9.37 | 60 | 13.9 | 8.87 |
| 100 | 288 | 9.34 | 100 | 9.5 | 8.97 |
| 100 | 300 | 9.35 | 100 | 15.3 | 9.09 |
| | | | 100 | 8.91 | 9.12 |

Related Ongoing Work

Researchers at the Colorado School of Mines (CSM), under contract to EG&G Rocky Flats, are performing extrusion optimization and relevant rheological studies.

Their efforts have been adjusted somewhat so as to rationally supplement (and not duplicate) the extrusion work done under the present ICO. This work is continuing.

A transient infrared (TIRS) monitor has been developed at Ames Laboratory and used to monitor nitrate concentrations on-line during extrusion. It was of interest to determine the accuracy of the monitor for a waste stream that was not IR-absorbing, *viz.* NaCl. Specimens from this study were provided to Ames (Stephan Weeks). The TIRS monitor accurately measured the NaCl loading of the processed waste stream, in real time, with a standard error of prediction of ±0.85 wt%.

Portions of the present study are being continued by LLNL in connection with the preliminary design of the Mixed Waste Management Facility (MWMF). Planned work includes LDPE microencapsulation of MSO filtered salt, and attempts to extrude with surfactants while maintaining acceptable extrusion rates. The "ash" from MSO and other treatment methods to be tested in MWMF are to be immobilized as a ceramic waste form. The successful immobilization of the ash is important, as it is expected to contain most of the radionuclides and RCRA metals. Ceramic waste form prepared from a surrogate MSO ash was of high quality and generally similar to specimens prepared from other surrogate residues. No processing difficulties developed (which had been the main concern). Some theoretical work intended to elucidate isolated aspects of microencapsulation waste form has also been undertaken.[8]

Performance Metric

Success for this task would be the provision of at least one final waste form that meets the waste acceptance criteria (WAC) of a landfill that will take the waste. If several forms meet this condition, then data useful for choosing between them for a given treatment environment should have been obtained or at least identified.

Results

TCLP leach results available at this time did not meet the necessary criteria for land disposal. However, our views on the advantages of this waste form for MSO salt remain unchanged: it provides a high-quality waste form with good salt loadings at reasonable costs. Twin-screw extrusion is technically preferable to single-screw, though more expensive. Good dispersion of the salt in the LDPE was achieved in this study. The inherent immobilization achievable by microencapsulation (i.e., ignoring any chemical pre-conditioning of the waste) requires further investigation. The effect of particle size will be evaluated when the remaining data of this project are in hand. The volumetric loading levels at which leach resistance began to deteriorate were disappointingly low. It is believed, however, that continued process innovation and optimization will lead to significantly better combinations of loading and immobilization.

---

[1]J. F. Cooper, internal memorandum, Lawrence Livermore National Laboratory, July 12, 1994.

[2]ASTM Standard D4212-93, "Standard Test Method for Viscosity by Dip-Type Viscosity Cups," ASTM Standards, Volume 06.01, 1993.

[3]G. J. Janz, "Thermodynamic and Transport Properties for Molten Salts: Correlation Equations for Critically Evaluated Density, Surface Tension, Electrical Conductance, and Viscosity Data," *Journal of Physical and Chemical Reference Data*, 17, 1988, Supplement No. 2, page 297.

[4]Janz, page 82.

[5]L. Abbey, M. McDowell, A. Darnell, R. Gay, K. Knudsen, and C. Newman, "Final Report for Molten Salt Oxidation of RMDF Mixed Wastes," Report Number 022-TR-0002, Energy Technology Engineering Center, Canoga Park, California, October 15, 1993.

[6]O. H. Krikorian, "Selection of Molten Salt Compositions for Bench-Scale Molten Salt Processor Tests," Report Number UCRL-ID-107091, Lawrence Livermore National Laboratory, April 1991.

[7]Janz, pages 141 (sodium chloride) and 144 (sodium carbonate).

[8] R. W. Hopper, LLNL internal reports and memoranda, in preparation.

[9]A. M. Faucette, *et al.*, EG&G Rocky Flats internal reports and memoranda, in preparation.

[10]A. M. Faucette, B. W. Logsdon & J. H. Oldham, "Review of the radioactive and thermal stability of low density polyethylene encapsulated nitrate salt waste." EG&G Rocky Flats internal report (8/7/92).

[11]P. D. Kalb, J. H. Heiser & P. Colombo, "Long-term durability of polyethylene for encapsulation of low-level radioactive, hazardous and mixed wastes," in *Emerging Technologies in Hazardous Waste Management,* D. W. Tedder & F. G. Pohland, Eds., American Chemical Society, 1993.

[12]A. Block-Bolten, D. Olson, P.-A. Persson & F. Sandstrom, "Polyethylene waste form evaluation of explosion and fire hazards." New Mexico Institute of Mining and Technology Center for Explosives Research report FR-91-03 (June 1991).

[13]P. D. Kalb, J. H. Heiser, III, & P. Colombo, "Polyethylene encapsulation of nitrate salt wastes: Waste form stability, process scale-up and economics." Brookhaven National Laboratory report BNL 52293 (July 1991).

[14]Private communication with Andrea Faucette, EG&G Rocky Flats, 11/94.

[15]R. C. Jantzen, D. M. Saiki, A. M. Faucette & D. L. Armentrout, "Evaluation of the effects of salt feed characteristics on polyethylene waste forms," EG&G Rocky Flats report TD-94-034 (Sept. 1994).

[16]A. M. Faucette, B. W. Logsdon & J. J. Lucerna, "Polymer solidifcation of secondary wastes from the fluid bed incineration unit." *Proceedings of the Mixed Waste Thermal Treatment Symposium* (U.S. DOE and EG&G Rocky Flats, Denver, April 1994).

[17]Private communications with Paul Kalb at Brookhaven National Laboratory, 10-11/94.

[18]See, for example, J. H. Oldham, A. M. Faucette, B. W. Hogsdon & R. J. Yudnich, "Treatability study of low level mixed Rocky Flats salt waste." EG&G Rocky Flats internal report no. TD-94-026 (9/30/94).

*Technical Information Department* • **Lawrence Livermore National Laboratory**
**University of California • Livermore, California 94551**